

BLOCKAGE DUE TO SUBREFLECTOR SUPPORTS IN LARGE
CASSEGRAIN RADIOTELESCOPEJ.W. Lamb and A. D. Olver
Queen Mary College, University of London, U.K.

In large Cassegrain antennas careful design is needed in order to minimise the detrimental effects on the antenna performance caused by blocking of the radiation by the subreflector supports. This paper reports a study on the aperture blocking effects by some possible support structures carried out for the United Kingdom/Netherlands 15 m Millimetrewave Telescope. This has very stringent mechanical specifications because of its very large size in wavelengths and the need to dynamically control the subreflector position. A mechanically good structure leads to poor electromagnetic performance with reduced aperture efficiency, increased sidelobes and increased noise temperature. The subreflector for the Millimetrewave Telescope is 750 mm in diameter and can be rocked at rates of up to 15 Hz to allow beam switching for atmospheric emission subtraction. The mass of the subreflector plus drive system for positioning and rocking is about 350 kg. The best support structure mechanically would have short and thick legs whereas minimal electrical blocking requires thin long legs which are attached to the edge of the main reflector. By examining the dependence of the blockage on the structural geometry and analysing the electrical performance an optimum structure was achieved. The standard tetrapod design used on many Cassegrain reflectors was abandoned in favour of an eight leg structure which has much better torsional strength, Fig. 1.

At millimetre wavelengths any support structure will have cross-sectional dimensions which are a number of wavelengths across so that a geometric optics analysis of their effects is sufficiently accurate for most purposes. Ray tracing may therefore be used to determine the shadow regions on the aperture. The rays are intercepted by a strut when propagating between the subreflector and the main reflector or when passing from the main reflector to the aperture. These two types correspond to blockage of a spherical wave and a plane wave respectively. In all practical cases a strut will intercept a given ray in either spherical wave blocking or plane wave blocking, but not both. The two types of blocking may therefore be treated independently. Fig. 2 shows the spherical and plane wave shadows on the aperture plane for a typical strut. The procedure for calculating these shadow regions involves computing the aperture coordinates of the rays grazing the edges of the struts over the aperture plane. This in general involves a numerical search procedure to find the solution to a set of coordinate transform equations. Two cross-sectional shapes for the struts were assumed, circular and elliptical.

Analytical expressions can be derived for the four leg structure of Fig. 1a. These enable the numerical procedure to be verified. Fig. 3 shows some results for this case. The dependence of the blockage on the angle of the legs to the antenna axis is clearly seen. When the top of the legs approach the subreflector edge the blockage rises sharply as the spherical wave blocking region widens at the edge of the aperture.

The eight leg structure of Fig. 1b must be studied numerically. It has a more complicated shadow pattern, Fig. 4, because the legs are inclined at angles to a radial direction. A parametric study of the effects of changing the lengths and positions of the three types of struts shown in Fig. 1b has been carried out. The main conclusion to be drawn from the computations of strut type A is that the strut should intersect the cone edge rays from the subreflector as far from the focus as possible so that the outer part of the spherical wave shadow does not become too large. The loss rises sharply as the legs come close to touching the subreflector edge. Struts B and C block only the plane wave. Their effect depends partly on the distribution of field across the aperture and hence on the edge taper. For a -20 dB taper the loss increases to a maximum and then decreases since there are two opposing effects: as the length increases, the geometrical area increases but the shadow moves to regions of lower field amplitude so that the weighting factor is reduced.

The total blocking for the eight leg support structure is shown in Fig. 5 as a function of the length of the top support structure. There is a broad minimum at 7.2 m which occurs when the plane wave shadows for the legs and the top square overlap each other. Although this minimum is lower than at 4 m, the top square has become rather large and flimsy so that the necessary increase in the width of the struts could offset the advantage of self shadowing.

The final design for the Millimetrewave Telescope uses an eight leg structure with a top dimension of 2.5 m. This is not the optimum solution electrically but is a good compromise with the mechanical constraints. The computed gain loss with a -10 dB edge taper is 7.4%. This compares with 5.0% for the best four leg structure. The extra 2.4% in loss is considered acceptable because of the mechanical superiority of the eight leg design.

As well as lowering the gain the blockage influences the sidelobe pattern. In order to compute these effects the radiation pattern was calculated by aperture integration. A grid of 64 by 64 points on the aperture was used and the field in each cell of the grid was weighted according to the fraction of the area blocked. In Fig. 6 the radiation patterns for no blocking and the eight leg structure are compared. Only minor changes in the sidelobe level occur. A standard tetrapod

produces much worse distortions because the four cones of scattered radiation reinforce in pairs near boresight. In the eight leg structure the scattered energy goes in a variety of directions and so is smeared out more uniformly.

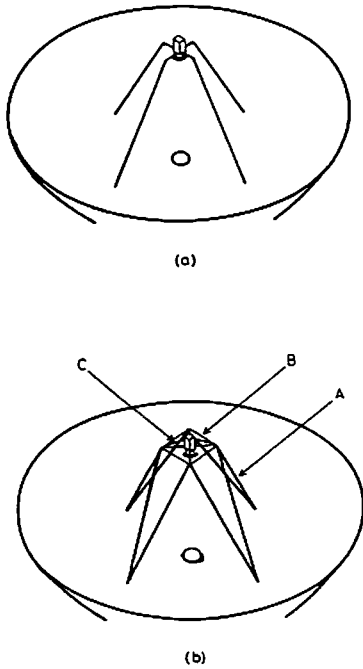


Fig. 1. Subreflector supports

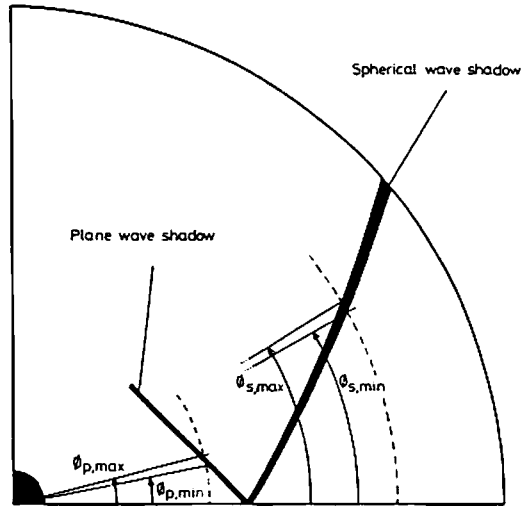


Fig. 2. Aperture shadow

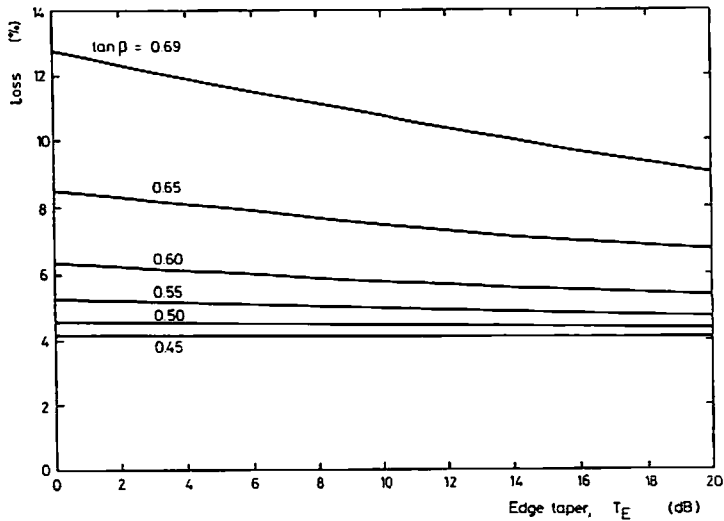


Fig. 3. Dependence of strut blocking on leg angle

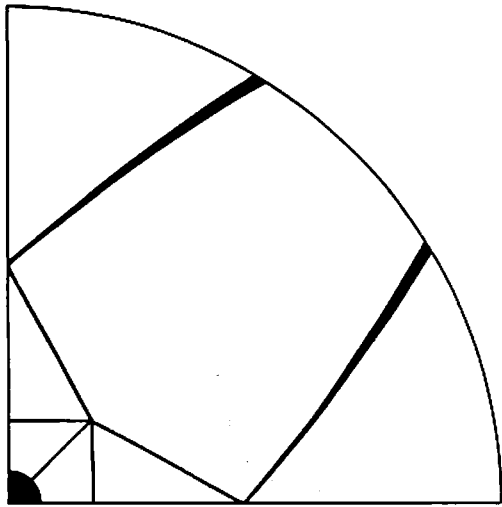


Fig. 4. Aperture shadow for eight leg design

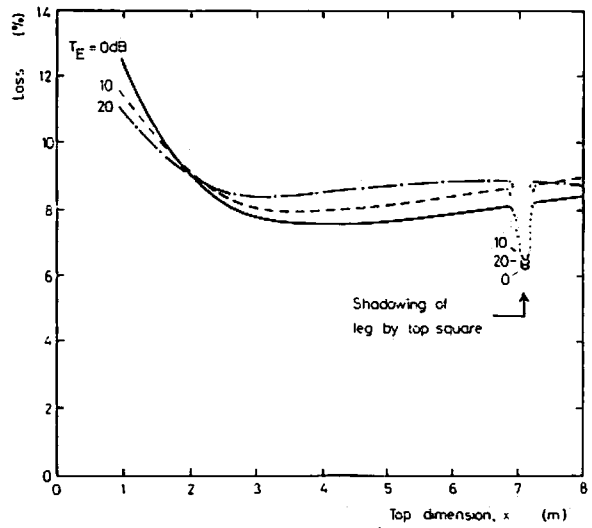


Fig. 5. Blocking loss

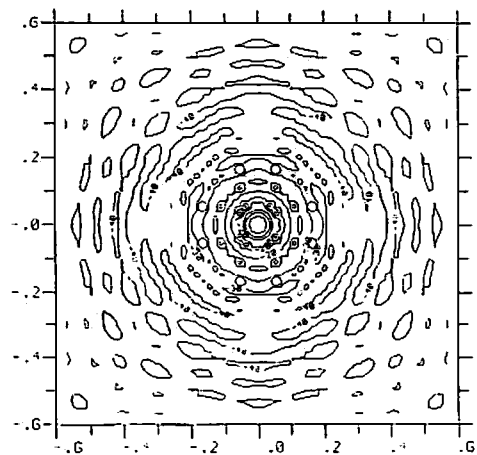
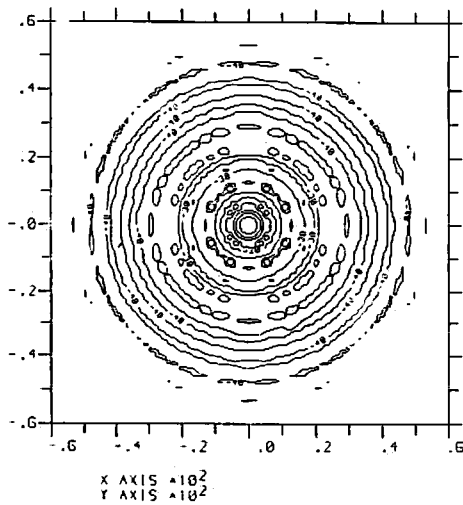


Fig. 6. Radiation patterns for no blocking and eight leg design